Morphological and molecular comparisons between tibialis anterior muscle and levator veli palatini muscle: A preliminary study on their augmentation potential

XU CHENG[1,2], LEI SONG[1,2], MIN LAN[1,2], BING SHI[1,2] and JINGTAO LI[1,2]

[1]Department of Oral and Maxillofacial Surgery; [2]State Key Laboratory of Oral Diseases, West China Hospital of Stomatology, Sichuan University, Chengdu, Sichuan 610041, P.R. China

Received April 9, 2017; Accepted September 14, 2017

DOI: 10.3892/etm.2017.5391

Abstract. Tibialis anterior (TA) muscle and other somite-derived limb muscles remain the prototype in skeletal muscle study. The majority of head muscles, however, develop from branchial arches and maintain a number of heterogeneities in comparison with their limb counterparts. Levator veli palatini (LVP) muscle is a deep-located head muscle responsible for breathing, swallowing and speech, and is central to cleft palate surgery, yet lacks morphological and molecular investigation. In the present study, multiscale *in vivo* analyses were performed to compare TA and LVP muscle in terms of their myofiber composition, *in-situ* stem cell population and augmentation potential. TA muscle was identified to be primarily composed of type 2B myofibers while LVP muscle primarily consisted of type 2A and 2X myofibers. In addition, LVP muscle maintained a higher percentage of centrally-nucleated myofibers and a greater population of satellite cells. Notably, TA and LVP muscle responded to exogenous Wnt7a stimulus in different ways. Three weeks after Wnt7a administration, TA muscle exhibited an increase in myofiber number and a decrease in myofiber size, while LVP muscle demonstrated no significant changes in myofiber number or myofiber size. These results suggested that LVP muscle exhibits obvious differences in comparison with TA muscle. Therefore, knowledge acquired from TA muscle studies requires further testing before being applied to LVP muscle.

Correspondence to: Dr Jingtao Li, Department of Oral and Maxillofacial Surgery, West China Hospital of Stomatology, Sichuan University, 14 Ren Min Nan Road, Chengdu, Sichuan 610041, P.R. China
E-mail: lijingtao86@163.com

Abbreviations: LVP, levator veli palatini; TA, tibia anterior

Key words: myogenesis, centrally-nucleated myofiber, satellite cell, myosin heavy chain isoform

Introduction

The human body possesses ~640 skeletal muscles, which account for ~40% of the whole body mass (1). These skeletal muscles are responsible for body movement and fulfill the functions of locomotion, respiration, swallowing and speech. Although they share the common architectural traits of striated muscles, the skeletal muscles have distinct embryonic origins (2). Trunk and limb muscles derive from somites; the majority of head muscles, such as masseter muscle and pharyngeal muscles, derive from branchial arches; extraocular muscles derive from prechordal mesoderm (3-5).

The prototype for skeletal muscle study is somite-derived limb muscles, but these represent only a small proportion of the whole skeletal muscle population (1). Investigations into head muscles have revealed that they exhibit heterogeneity in comparison with their limb counterparts. During embryonic myogenesis, T-box 1 and pituitary homeobox 2 mediate the formation of head muscles, yet are absent in limb muscle development (4,6). Head muscles possess a visceral mesodermal origin and are closely associated with heart development in myogenesis (7,8). Mesoderm in the cardiopharyngeal field gives rise to both the branchiomeric muscles and part of the heart (3). In addition, masseter muscle was reported to regenerate less effectively compared with tibialis anterior (TA) muscle (9). These results point to the notion that head muscles and limb muscles are markedly different skeletal muscle populations.

TA muscle has been studied extensively, particularly its developmental origin, morphological characteristics and augmentation potential (9-11). Levator veli palatini (LVP) muscle, however, lacks investigation in spite of its critical role in fulfilling velopharyngeal function and its core status in cleft palate surgery (12-14). Plastic surgeons have long been searching for strategies to augment LVP muscle, in order to facilitate velopharyngeal closure and improve speech in patients with cleft palates (15-17).

Strategies for muscle augmentation have been sought for decades. Effective agents, such as insulin-like growth factor (IGF)-1, angiotensin and Wnt7a, have previously been proposed to increase myofiber diameter and enhance muscle function in atrophied or normal muscle (10,18-20). These studies were primarily performed in limb muscles like the

TA muscle. Considering the general differences between limb and head muscle, combined with the knowledge gap for LVP muscle augmentation, the present study was performed for two reasons: i) To glean background information of LVP muscle, in comparison with TA muscle; ii) to investigate whether the two muscles exhibited different augmentation potential. In the present study, the differences between TA and LVP muscle were characterized in terms of muscle fiber composition, *in situ* stem cell population and activation level of the Wnt signaling pathway under basal conditions. Furthermore, it was investigated whether the two muscles responded differently to growth factor stimulus.

Materials and methods

Animals. All experimental procedures on animals were approved by the Institutional Animal Care and Use Committee at Sichuan University (Chengdu, China). Adult male Sprague-Dawley rats (age, 10 weeks; weight, 280-300 g) were purchased from Chengdu Dashuo Experimental Animal Center (Chengdu, China). The animals were raised in a temperature- and humidity-controlled room (temperature, 21±2˚C; relative humidity, 50±5%) on a 12-h light/dark schedule. Food and water were freely accessible. A total of 18 animals were used in the present study and were randomly allocated to the following three groups: i) comparison between TA muscle and LVP muscle under basal conditions (n=6); ii) intramuscular Wnt7a administration of TA muscle (n=6); iii) intramuscular Wnt7a administration of LVP muscle (n=6).

Intramuscular Wnt7a delivery. Recombinant human Wnt7a (R&D Systems, Inc., Minneapolis, MN, USA) was injected directly into the muscles. For each TA muscle (n=6), 75 μl Wnt7a (100 μg/ml) was injected and 75 μl PBS was injected to the TA muscle in the contralateral leg as control; for each LVP muscle (n=6), 25 μl Wnt7a (100 μg/ml) was injected and 25 μl PBS was injected to the LVP muscle on the contralateral side as control. Injection into LVP muscle was carried out via an intraoral procedure. Rats were sacrificed 3 weeks after treatment and muscles were harvested for analyses.

Muscle harvest. TA muscle was cut from tendon to tendon on the tibia anterior bone. LVP muscle was approached and isolated according to Carvajal Monroy *et al* (21), with small modifications. Briefly, a ventral incision extending from the mandibular symphysis to the clavicle was made and the subcutaneous tissue was separated to expose the salivary gland. After removal of the salivary gland, the digastric and sternocleidomastoid muscle was visible. The posterior belly of the digastric muscle was dissected to its origin to expose the stylohyoid muscle beneath it and the tympanic bulla. The stylohyoid muscle was cut at its junction to the hyoid and pulled laterally to visualize the LVP muscle with its tendon clearly attached to the tympanic bulla. The LVP muscle was carefully dissected from its origin in the tympanic bulla to its insertion in the soft palate.

Immunofluorescence analysis. Muscle samples were attached to the chuck using Tissue-Tek Optimal Cutting Temperature compound (Sakura Finetek USA, Inc., Torrance, CA, USA) and frozen in isopentane cooled with liquid nitrogen using Lawlor's method (22). Cryosections were made at 10 μm thickness and fixed in 0˚C acetone (100%) for 20 min. The sections were dried at room temperature for 20 min and washed in 0.01 mol/l phosphate-buffered saline (PBS). Sections were then blocked with PBS containing 5% bovine serum albumin (Amresco, LLC, Solon, OH, USA), and 5% donkey serum (Beijing Solarbio Science & Technology Co., Ltd., Beijing, China) for 1 h at 25˚C, and subsequently incubated overnight at 4˚C with primary antibodies. Following washing in PBS, sections were incubated for 1 h at 25˚C with Alexa Fluor 488-conjugated (A-21206; 1:500) and 568-conjugated (A10037; 1:500) secondary antibodies (Invitrogen; Thermo Fisher Scientific, Inc., Waltham, MA, USA). After several washes in PBS, the nuclei were stained with DAPI. Images were captured with an Olympus BX63 fluorescence microscope (Olympus Corporation, Tokyo, Japan). The primary antibodies used were as follows: Rabbit anti-laminin polyclonal antibody (L9393; 1:500; Sigma-Aldrich; Merck KGaA, Darmstadt, Germany), mouse anti-Pax7 monoclonal antibody (PAX7; 1:5; Developmental Studies Hybridoma Bank, Iowa City, IA, USA), rabbit anti-Ki67 monoclonal antibody (ab1667; 1:500; Abcam, Cambridge, MA, USA), mouse anti-myosin heavy chain 1 (MyHC-1) monoclonal antibody (A4.840; 1:40; Developmental Studies Hybridoma Bank), mouse anti-MyHC-2A monoclonal antibody (SC-71; 1:20; Developmental Studies Hybridoma Bank), mouse anti-MyHC-2X monoclonal antibody (6H1; 1:5; Developmental Studies Hybridoma Bank) and mouse anti-MyHC-2B monoclonal antibody (BF-F3; 1:5; Developmental Studies Hybridoma Bank).

Western blot analysis. Muscle samples were minced and prepared in RIPA lysis buffer (Beyotime Institute of Biotechnology, Haimen, China). Tissues were incubated for 30 min on ice, followed by centrifugation at 12,000 x g for 10 min at 4˚C. Total protein concentration in the supernatant was determined using a BCA protein assay kit (Beijing Solarbio Science & Technology Co., Ltd.). Protein extract (7 μl/lane) was loaded on 10% SDS-PAGE and transferred onto polyvinylidene fluoride membranes (EMD Millipore, Billerica, MA, USA). After blocking with 5% bovine serum albumin in 0.5% TBS-Tween-20 at room temperature for 1 h, the membranes were incubated with primary antibodies at 4˚C overnight. Then, the membranes were incubated with horseradish peroxidase-conjugated secondary antibody for 1 h at 37˚C. The protein bands were visualized using an enhanced chemiluminescence system (G2014; Wuhan Goodbio Technology Co., Ltd., Wuhan, China). Densitometry values were normalized to the intensity of corresponding bands for GAPDH. Quantitative analysis of western blotting was performed using ImageJ version 1.50e (National Institutes of Health, Bethesda, MD, USA). Primary antibodies were used as follows: Rabbit polyclonal anti-Axin2 antibody (ab32197; 1:1,000; Abcam), sheep polyclonal anti-Vangl2 antibody (AF4815; 1:1,000; R&D Systems, Inc.), rabbit polyclonal anti-pS6 antibody (2211; 1:1,000; Cell Signaling Technology, Inc., Danvers, MA, USA), rabbit polyclonal anti-pAkt antibody (9271; 1:1,000, Cell Signaling Technology, Inc.) and rabbit polyclonal anti-GAPDH antibody (ab9485; 1:1,000; Abcam). Secondary antibodies were used as follows: Goat anti-rabbit

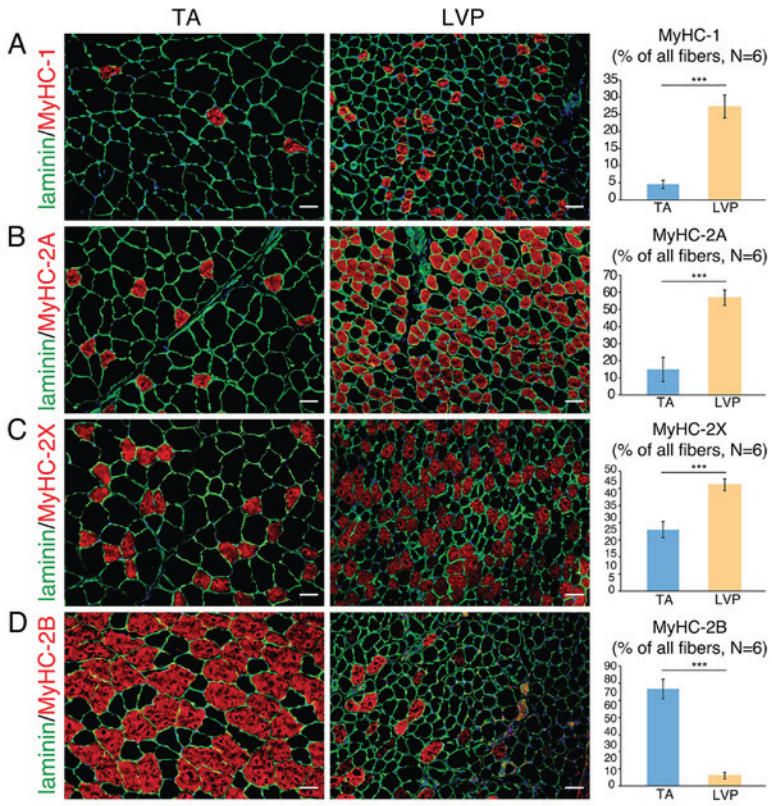

Figure 1. Muscle fiber types in TA and LVP muscle. (A) Immunofluorescence staining of MyHC-1 (red) and laminin (green). Quantification of MyHC-1 is indicated on the right panel. (B) Immunofluorescence staining of MyHC-2A (red) and laminin (green), Quantification of MyHC-2A is indicated on the right panel. (C) Immunofluorescence staining of MyHC-2X (red) and laminin (green). Quantification of MyHC-2X is indicated on the right panel. (D) Immunofluorescence staining of MyHC-2B (red) and laminin (green). Quantification of MyHC-2B is indicated on the right panel. Scale bar=50 μm. ***P<0.001 as indicated. TA, tibialis anterior; LVP, levator veli palatini; MyHC, myosin heavy chain.

IgG (ab6721; 1:5,000; Abcam) and donkey anti-sheep IgG (ab97125; 1:5,000; Abcam).

Quantification and statistical analyses. Myofiber size and overall cell density were calculated using ImageJ 1.50e. Numbers of Pax7-positive nuclei, Ki67-positive nuclei and the percentage of each specific fiber type were manually counted with three fields of view selected for each sample type. All data were analyzed using SPSS 19.0 (IBM Corp., Armonk, NY, USA) and results are presented as the mean ± standard deviation. Student's t-test was used to evaluate statistical differences. P<0.05 was considered to indicate a statistically significant difference.

Results

Fiber type composition of TA and LVP muscle. Sections of muscle samples revealed that individual fibers in TA muscle were larger compared with LVP muscle (data not shown). With their corresponding markers immunostained, different types of muscle fibers were identified and quantified in TA and LVP muscle. The percentage of MyHC-1 fibers was significantly higher in LVP muscle compared with TA muscle (~25 vs. ~5%; Fig. 1A). The percentage of MyHC-2A fibers was significantly higher in LVP muscle compared with TA muscle (~60 vs. ~15%; Fig. 1B). The percentage of MyHC-2X fibers was significantly higher in LVP muscle compared with TA muscle (~40 vs. ~25%; Fig. 1C). By contrast, the percentage of MyHC-2B fibers was significantly higher in TA muscle compared with LVP muscle (~75 vs. ~5%; Fig. 1D). These results indicated that the vast majority of TA muscle is composed of type 2B fibers, while the majority of fibers in LVP muscle are types 2A and 2X.

Satellite cells and centrally-nucleated myofibers in TA and LVP muscle. The number of nuclei per area was significantly higher in LVP muscle compared with TA muscle (Fig. 2A). The number of Pax7-positive nuclei, an indicator of satellite cells, was significantly higher in LVP muscle compared with TA muscle (~2.2% vs. ~0.3%; Fig. 2B). Satellite cells are resident stem cells in skeletal muscle tissue, wedged in the interspace between sarcolemma and basal lamina (23). When activated, satellite cells proliferate and differentiate either to merge into pre-existing fibers or form new fibers, distinguishing the involved myofibers as centrally-nucleated myofibers (24). In TA muscle, centrally-nucleated myofibers were only scarcely identified (~0.1% of total fibers), but they were observed significantly more frequently in LVP muscle (~1.5% of total fibers; Fig. 2C). These data suggested that LVP muscle possesses a broader stem cell pool and more active myonuclei turnover compared with TA muscle. Given that Wnt signaling is closely associated with satellite cell activity (25), further investigation was performed in the Wnt pathway.

Wnt signaling hubs in TA muscle and LVP muscle. In canonical Wnt pathways, Axin2 is a direct target gene

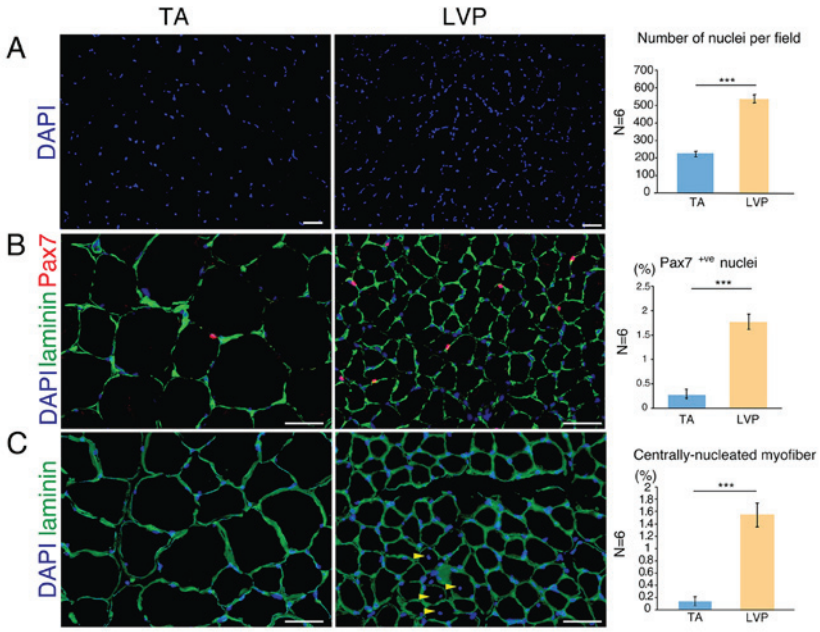

Figure 2. Distribution of satellite cells and centrally-nucleated myofibers in TA and LVP muscle. (A) DAPI staining of muscle sections from TA muscle and LVP muscle. Quantification of total nuclei per field is indicated on the right panel. (B) Immunofluorescence staining of laminin (green), Pax7 (red) and DAPI (blue) in TA and LVP muscle. Quantification of Pax7-positive nuclei is indicated on the right panel. (C) Immunofluorescence staining of laminin (green) and DAPI (blue). Yellow arrowheads indicate centrally-nucleated myofibers. Quantification of centrally-nucleated myofibers is indicated on the right panel. Scale bar=50 μm. ***P<0.001 as indicated. TA, tibialis anterior; LVP, levator veli palatini.

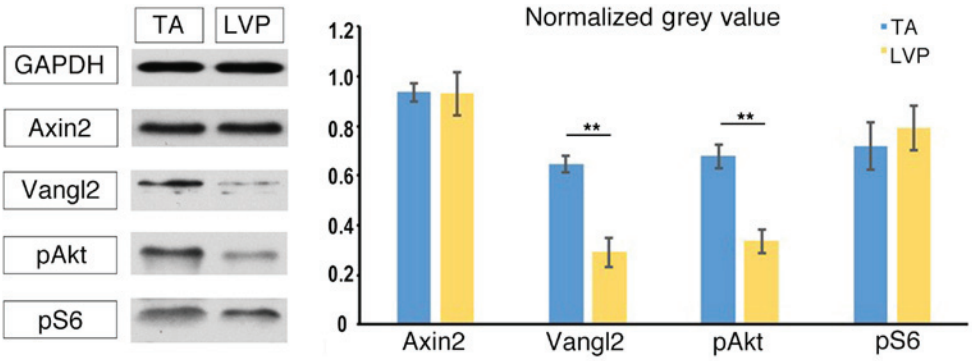

Figure 3. Protein analysis of Wnt signaling hubs in TA and LVP muscle. Blots of Axin2, Vangl2, pAkt, pS6 and their densitometric analyses are indicated. All values were normalized to GAPDH levels. **P<0.01 as indicated. TA, tibialis anterior; LVP, levator veli palatini.

of Wnt and its expression is a reliable marker for the activation of Wnt signaling (26). For non-canonical Wnt pathways, the expression of Vangl2 reflects the activation of Wnt/planar cell polarity pathway (27), while pAkt and pS6 are indicators of Wnt/Akt/mechanistic target of rapamycin pathway activation (10). No significant differences were identified in the expression of Axin2 between TA muscle and LVP muscle (Fig. 3). The expression level of Vangl2 was observed to be significantly higher in TA muscle compared with LVP muscle (Fig. 3). Similarly, pAkt was expressed at a significantly higher level in TA muscle compared with LVP muscle (Fig. 3). No significant differences were identified in the expression of pS6 between TA muscle and LVP muscle (Fig. 3). Based on these differences in the baseline level of Wnt hubs, it was investigated whether LVP and TA muscle responded differently to Wnt ligand stimulus.

TA and LVP muscles respond differently to exogenous Wnt7a stimulus. Wnt7a has been demonstrated to be effective in expanding TA muscles (10,28), but to the best of our knowledge, has not been tested in LVP muscle before. At 3 weeks after a single injection of recombinant Wnt7a protein, TA and LVP muscles were harvested for comparison. After Wnt7a administration, the percentage of Ki67-positive nuclei, which indicated proliferative cells, increased significantly in TA and LVP muscle (Fig. 4A and B). The two muscle types exhibited a marked increase in centrally-nucleated myofibers after Wnt7a administration (Fig. 4C). Notably, in TA muscle, a significant increase in myofibers was observed after Wnt7a injection, leading to a five-fold increase in the number of myofibers and a significant decrease in the average myofiber size (Fig. 4C and D). In LVP muscle, however, the number and the average size of the myofibers stayed constant after Wnt7a administration (Fig. 4C and E).

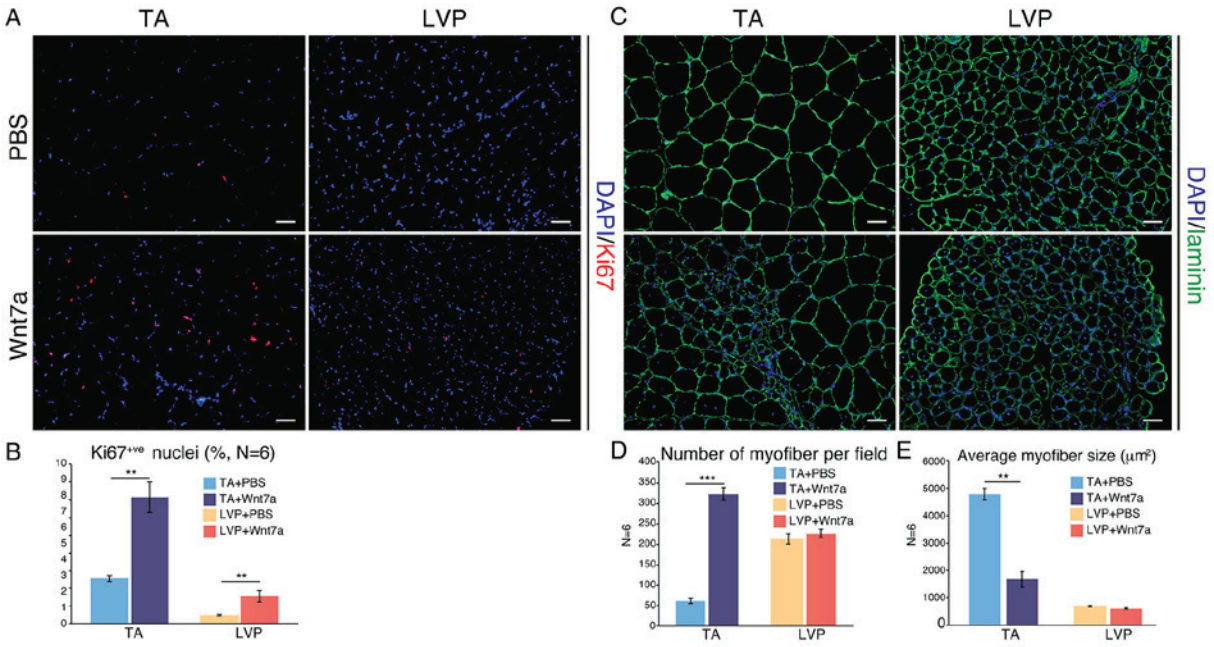

Figure 4. Effect of exogenous Wnt7a stimulus on TA and LVP muscle. (A) Immunofluorescence staining of Ki67 (red) and DAPI (blue) in tissue sections from TA or LVP muscle treated with PBS or Wnt7a. (B) Quantification of Ki67-positive nuclei. (C) Immunofluorescence staining of laminin (green), and DAPI (blue) in tissue sections from TA or LVP muscle treated with PBS or Wnt7a. (D) Quantification of the number of myofibers per field with and without Wnt7a treatment. (E) Quantification of myofiber size with and without Wnt7a treatment. **P<0.01, ***P<0.001 as indicated. Scale bar=50 μm. TA, tibialis anterior; LVP, levator veli palatini.

Discussion

From the perspective of embryonic origin, TA and LVP muscle fall into different categories: TA muscle derives from somites (2), while LVP muscle derives from the fourth and sixth branchial arches (13). Apart from their differences in embryonic origin, the current study has characterized further heterogeneities between the two muscle types.

Until now, the predominant model of fiber types has been based on four major MyHC isoforms: MyHC-1, -2A, -2X and -2B (29). From type 1 to type 2B fibers, the shortening velocity gradually increases and resistance to fatigue decreases (29). The composition of different fiber types is closely associated with the muscle function. Specifically, TA muscle is more suitable for fast and powerful actions such as jumping and kicking, while LVP muscle is streamlined for slower contractions with longer durations in elevating and stretching the soft palate (30,31). Consequently, it was identified in the present study that TA muscle is largely composed of MyHC-2B myofibers, while LVP muscle primarily consists of MyHC-2A and MyHC-2X fibers. Hybrid fibers co-expressing different MyHC isoforms are common (29), since boundaries between different fiber types are not clear. This could explain why the sum of all four MyHC isoforms in the muscles was >100%. Apart from gleaning baseline information of fiber type composition in the two specific muscles, the data presented here could also be relevant to clinical practice. Fiber type composition can have profound impacts on the specific muscle's susceptibility to disease. For example, type 2 fibers are preferentially affected in Duchenne muscular dystrophy (DMD), and inducing type 1 fibers can ameliorate DMD (32).

Satellite cells are well-recognized resident stem cells within skeletal muscle tissue (23). It was revealed in the present study that LVP muscle maintains a higher satellite cell content compared with TA muscle. During muscle repair or regeneration, satellite cells undergo asymmetric division and differentiate into myogenic progenitors, either fusing into the existing myofibers or becoming *de novo* myofibers (33). In this process, the involved myofibers are distinguished as centrally-nucleated myofibers. It has long been speculated that satellite cells remain quiescent in their sublaminar niche until required for skeletal muscle repair (23,25,33). However, recent studies performed by Randolph *et al* (34) and Keefe *et al* (35) have demonstrated that satellite cells contribute nuclei to myofibers in adult muscles in sedentary mice, challenging this conventional view. Similarly, in the present study, satellite cell activity in 2-month-old rat skeletal muscle was detected under basal conditions, as evidenced by the presence of centrally-nucleated myofibers. It was also identified that the percentage of centrally-nucleated myofibers was significantly higher in LVP muscle compared with TA muscle. With regards to the core components in Wnt signaling, protein analyses revealed that Vangl2 and pAkt are expressed at a higher level in TA muscle compared with LVP muscle. These molecular differences indicated different Wnt pathway activation levels under basal conditions in TA muscle and LVP muscle. However, the mechanisms underlying the broader stem cell pool and more active myonuclei turnover in LVP are yet to be elucidated.

In the present study, it was further examined whether TA and LVP muscle responded differently to exogenous myogenic growth factor. Wnt7a was selected because it was less likely to induce resistance to growth hormone or cause hypoglycemia,

when compared with IGF-1 (10). Previous studies by von Maltzahn *et al* (10,28) have indicated the key role of recombinant Wnt7a protein in augmenting mouse limb muscle, leading to significant myofiber hypertrophy and enhanced muscle function. Notably, there were two primary findings in the present study. First, Wnt7a induced hyperplasia rather than hypertrophy in TA muscle. This discrepancy may be attributed to the different postnatal growth patterns in muscle fibers between mice and rats. Typically, the number of myofibers remains constant after birth in mice, while the number and size of myofibers continue to increase for 10 weeks in rats (20,36). Secondly, TA and LVP muscle reflected different augmentation potential after Wnt7a delivery. In TA muscle, the number of myofibers increased significantly, a large proportion of which were observed to be centrally-nucleated myofibers. However, LVP muscle did not exhibit an increase in myofiber number, despite markedly upregulating the number of centrally-located myofibers. The two muscle types exhibited augmentation potential in response to Wnt7a stimulus, but had different responses. The reason for these differences requires further investigation.

LVP muscle was selected for investigation in the current study primarily due to its clinical significance. LVP muscle elevates the soft palate and serves a critical function in velopharyngeal closure. Reduced LVP muscle volume and compromised LVP muscle function in patients with cleft palate results in affected speech (12). Effective augmentation of LVP muscle via biological therapeutics may revolutionize the management of cleft palate.

The present study has certain limitations. The newly-formed myofibers with small diameters observed in TA muscle 3 weeks after Wnt7a administration were immature. To probe the augmentation effect, a longer observation time is required in order to assess the development of these new fibers. In addition, the notable discrepancies between the responses of TA and LVP muscle to Wnt7a administration highlights the requirement for more in-depth work in order to reveal the underlying mechanisms.

In conclusion, LVP muscle is distinct from TA muscle in its myofiber composition, *in-situ* stem cell population, Wnt signaling hub expression and augmentation potential. Therefore, therapeutics that are effective in TA muscle may not be effective in LVP muscle, and further studies are required in order to elucidate the differences between the muscle types.

Acknowledgements

This study was supported by grants from the National Natural Science Foundation of China to Dr Jingtao Li (grant no. 81500829) and Professor Bing Shi (grant no. 81470729).

References

1. Randolph ME and Pavlath GK: A muscle stem cell for every muscle: Variability of satellite cell biology among different muscle groups. Front Aging Neurosci 7: 190, 2015.
2. Sambasivan R, Kuratani S and Tajbakhsh S: An eye on the head: The development and evolution of craniofacial muscles. Development 138: 2401-2415, 2011.
3. Diogo R, Kelly RG, Christiaen L, Levine M, Ziermann JM, Molnar JL, Noden DM and Tzahor E: A new heart for a new head in vertebrate cardiopharyngeal evolution. Nature 520: 466-473, 2015.
4. Kelly RG: Core issues in craniofacial myogenesis. Exp Cell Res 316: 3034-3041, 2010.
5. Michailovici I, Eigler T and Tzahor E: Craniofacial muscle development. Curr Top Dev Biol 115: 3-30, 2015.
6. Shih HP, Gross MK and Kioussi C: Cranial muscle defects of Pitx2 mutants result from specification defects in the first branchial arch. Proc Natl Acad Sci USA 104: 5907-5912, 2007.
7. Grifone R and Kelly RG: Heartening news for head muscle development. Trends Genet 23: 365-369, 2007.
8. Tzahor E and Evans SM: Pharyngeal mesoderm development during embryogenesis: Implications for both heart and head myogenesis. Cardiovasc Res 91: 196-202, 2011.
9. Pavlath GK, Thaloor D, Rando TA, Cheong M, English AW and Zheng B: Heterogeneity among muscle precursor cells in adult skeletal muscles with differing regenerative capacities. Dev Dyn 212: 495-508, 1998.
10. von Maltzahn J, Bentzinger CF and Rudnicki MA: Wnt7a-Fzd7 signalling directly activates the Akt/mTOR anabolic growth pathway in skeletal muscle. Nat Cell Biol 14: 186-191, 2012.
11. Stuelsatz P, Shearer A, Li Y, Muir LA, Ieronimakis N, Shen QW, Kirillova I and Yablonka-Reuveni Z: Extraocular muscle satellite cells are high performance myo-engines retaining efficient regenerative capacity in dystrophin deficiency. Dev Biol 397: 31-44, 2015.
12. Fisher DM and Sommerlad BC: Cleft lip, cleft palate, and velopharyngeal insufficiency. Plast Reconstr Surg 128: 342e-360e, 2011.
13. Cohen SR, Chen L, Trotman CA and Burdi AR: Soft-palate myogenesis: A developmental field paradigm. Cleft Palate Craniofac J 30: 441-446, 1993.
14. Koch KH, Grzonka MA and Koch J: The pathology of the velopharyngeal musculature in cleft palates. Ann Anat 181: 123-136, 1999.
15. Carvajal Monroy PL, Grefte S, Kuijpers-Jagtman AM, Wagener FA and Von den Hoff JW: Strategies to improve regeneration of the soft palate muscles after cleft palate repair. Tissue Eng Part B Rev 18: 468-477, 2012.
16. Iwata J, Suzuki A, Yokota T, Ho TV, Pelikan R, Urata M, Sanchez-Lara PA and Chai Y: TGFβ regulates epithelial-mesenchymal interactions through WNT signaling activity to control muscle development in the soft palate. Development 141: 909-917, 2014.
17. Crockett DJ and Goudy SL: Update on surgery for velopharyngeal dysfunction. Curr Opin Otolaryngol Head Neck Surg 22: 267-275, 2014.
18. Chakravarthy MV, Bradley SD and Frank WB: IGF-1 restores satellite cell proliferation potential in immobilized old skeletal muscle. J Appl Physiol (1985) 89: 1365-1379, 2000.
19. Márquez-Miranda V, Abrigo J, Rivera JC, Araya-Durán I, Aravena J, Simon F, Pacheco N, González-Nilo FD and Cabello-Verrugio C: The complex of PAMAM-OH dendrimer with Angiotensin (1-7) prevented the disuse-induced skeletal muscle atrophy in mice. Int J Nanomedicine 12: 1985-1999, 2017.
20. White RB, Bierinx AS, Gnocchi VF and Zammit PS: Dynamics of muscle fibre growth during postnatal mouse development. BMC Dev Biol 10: 21, 2010.
21. Carvajal Monroy PL, Grefte S, Kuijpers-Jagtman AM, Helmich MP, Ulrich DJ, Von den Hoff JW and Wagener FA: A rat model for muscle regeneration in the soft palate. PLoS One 8: e59193, 2013.
22. Meng H, Janssen PM, Grange RW, Yang L, Beggs AH, Swanson LC, Cossette SA, Frase A, Childers MK, Granzier H, *et al*: Tissue triage and freezing for models of skeletal muscle disease. J Vis Exp, 2014.
23. Chang NC and Rudnicki MA: Satellite cells: The architects of skeletal muscle. Curr Top Dev Biol 107: 161-181, 2014.
24. Cadot B, Gache V and Gomes ER: Moving and positioning the nucleus in skeletal muscle-one step at a time. Nucleus 6: 373-381, 2015.
25. Dumont NA, Bentzinger CF, Sincennes MC and Rudnicki MA: Satellite cells and skeletal muscle regeneration. Compr Physiol 5: 1027-1059, 2015.
26. Huraskin D, Eiber N, Reichel M, Zidek LM, Kravic B, Bernkopf D, von Maltzahn J, Behrens J and Hashemolhosseini S: Wnt/β-catenin signaling via Axin2 is required for myogenesis and, together with YAP/Taz and Tead1, active in IIa/IIx muscle fibers. Development 143: 3128-3142, 2016.
27. Le Grand F, Jones AE, Seale V, Scimè A and Rudnicki MA: Wnt7a activates the planar cell polarity pathway to drive the symmetric expansion of satellite stem cells. Cell Stem Cell 4: 535-547, 2009.

28. von Maltzahn J, Renaud JM, Parise G and Rudnicki MA: Wnt7a treatment ameliorates muscular dystrophy. Proc Natl Acad Sci USA 109: 20614-20619, 2012.
29. Schiaffino S and Reggiani C: Fiber types in mammalian skeletal muscles. Physiol Rev 91: 1447-1531, 2011.
30. Perry JL, Kuehn DP and Sutton BP: Morphology of the levator veli palatini muscle using magnetic resonance imaging. Cleft Palate Craniofac J 50: 64-75, 2013.
31. Lindman R, Paulin G and Stål PS: Morphological Characterization of the levator veli palatini muscle in children born with cleft palates. Cleft Palate Craniofac J 38: 438-448, 2001.
32. Talbot J and Maves L: Skeletal muscle fiber type: Using insights from muscle developmental biology to dissect targets for susceptibility and resistance to muscle disease. Wiley Interdiscip Rev Dev Biol 5: 518-534, 2016.
33. Yin H, Price F and Rudnicki MA: Satellite cells and the muscle stem cell niche. Physiol Rev 93: 23-67, 2013.
34. Randolph ME, Phillips BL, Choo HJ, Vest KE, Vera Y and Pavlath GK: Pharyngeal satellite cells undergo myogenesis under basal conditions and are required for pharyngeal muscle maintenance. Stem Cells 33: 3581-3595, 2015.
35. Keefe AC, Lawson JA, Flygare SD, Fox ZD, Colasanto MP, Mathew SJ, Yandell M and Kardon G: Muscle stem cells contribute to myofibres in sedentary adult mice. Nat Commun 6: 7087, 2015.
36. Tamaki T, Akatsuka A, Yorshimura S, Roy RR and Edgerton VR: New fiber formation in the interstitial spacs of rat skeletal muscle during postnatal growth. J Histochem Cytochem 50: 1097-1111, 2002.